Food Chemistry 181 (2015) 133–139

Contents lists available at ScienceDirect

Food Chemistry

journal homepage: www.elsevier.com/locate/foodchem

# Modification of porous starch for the adsorption of heavy metal ions from aqueous solution

Xiaofei Ma [a], Xueyuan Liu [a], Debbie P. Anderson [b], Peter R. Chang [b,c,*]

[a] School of Science, Tianjin University, Tianjin 300072, China
[b] Bioproducts and Bioprocesses National Science Program, Agriculture and Agri-Food Canada, 107 Science Place, Saskatoon, SK S7N 0X2, Canada
[c] Department of Chemical and Biological Engineering, University of Saskatchewan, Saskatoon, SK S7N 5A9, Canada

ARTICLE INFO

*Article history:*
Received 20 October 2014
Received in revised form 16 February 2015
Accepted 17 February 2015
Available online 24 February 2015

*Keywords:*
Porous starch
Adsorption
Starch xanthate
Starch citrate
Starch modification
Heavy metal ions

ABSTRACT

Porous starch xanthate (PSX) and porous starch citrate (PSC) were prepared in anticipation of the attached xanthate and carboxylate groups respectively forming chelation and electrostatic interactions with heavy metal ions in the subsequent adsorption process. The lead(II) ion was selected as the model metal and its adsorption by PSX and PSC was characterized. The adsorption capacity was highly dependent on the carbon disulfide/starch and citric acid/starch mole ratios used during preparation. The adsorption behaviors of lead(II) ion on PSXs and PSCs fit both the pseudo-second-order kinetic model and the Langmuir isotherm model. The maximum adsorption capacity from the Langmuir isotherm equation reached 109.1 and 57.6 mg/g for PSX and PSC when preparation conditions were optimized, and the adsorption times were just 20 and 60 min, respectively. PSX and PSC may be used as effective adsorbents for removal of heavy metals from contaminated liquid.



## 1. Introduction

When heavy metals from various industrial activities enter aquatic systems, they must be removed from the wastewater because of their significant threat to human health. Among the various techniques used for treatment of heavy metals in wastewater, adsorption is a promising alternative due to ease of handling, low operating costs, high efficiency for removing very low levels of heavy metals from dilute solutions, and there is no threat of secondary contamination.

There are many adsorbents that can be used to remove heavy metals from aqueous solutions including oxidized carbon nanotubes (Tofighy & Mohammadi, 2011), graphene oxide (Wang, Yuan, et al., 2013), clay (Sdiri, Higashi, Chaabouni, & Jamoussi, 2012), and biomass sources (Altun & Pehlivan, 2012; Jain, Garg, & Kadirvelu, 2009; Kaya, Pehlivan, Schmidt, & Bahadie, 2014; Wang, Yin, et al., 2013). Natural polysaccharide-based adsorbents have been focused on because of their low cost, availability, and biodegradability. The building blocks of biomass-based polysaccharides have a substantial number of reactive hydroxyl, carboxyl, and/or amino groups that can be further modified for the removal of heavy metals. For example, a magnetic chitosan adsorbent was synthesized by surface modification of chitosan/$SiO_2$/$Fe_3O_4$ with EDTA using 3-ethyl-1-(3-dimethylaminopropyl) carbodiimide hydrochloride as the crosslinker in a buffer solution (Ren, Abbood, He, Peng, & Huang, 2013). This adsorbent could be collected using a magnetic separation process after $Cu^{2+}$, $Cd^{2+}$ and $Pb^{2+}$ were removed from the solution. In another study, a hybrid gel fabricated by crosslinking calcium alginate and gamma-poly glutamic acid was used to adsorb $Nd^{3+}$ (Wang et al., 2014). In addition, carboxylic acid functionalized deacetylated konjac glucomannan was used to remove heavy metals from water (Liu, Luo, Lin, Liang, & Chen, 2009). Meanwhile, cellulose xanthogenates derived from straw were prepared for use as adsorbents of heavy metals by sulfonation and magnesium substitution (Deng et al., 2012). Additionally, crosslinked amino starch was obtained by reacting ethylenediamine with dialdehyde starch for the adsorption of $Cu^{2+}$ and $Cr^{6+}$ (Dong et al., 2010).

Among biomass-based polysaccharides, starch and cellulose are the most promising raw materials with low cost and universality. During conventional modification of starch or cellulose, strong acid or base at high concentration is commonly used to destroy the intermolecular hydrogen bond interactions and crystallization regions, which then facilitates the chemical reaction between the starch and modifiers. Conversely, we postulate that porous starch (PS) with a large specific surface area and low crystallinity could foster effective modification under moderate reactive conditions

* Corresponding author at: Bioproducts and Bioprocesses National Science Program, Agriculture and Agri-Food Canada, 107 Science Place, Saskatoon, SK S7N 0X2, Canada. Tel.: +1 306 385 9449; fax: +1 306 385 9482.

*E-mail address:* peter.chang@agr.gc.ca (P.R. Chang).

http://dx.doi.org/10.1016/j.foodchem.2015.02.089
0308-8146/

while maintaining the porous structure. We believe that the porous starch xanthate (PSX) and porous starch citrate (PSC) prepared here have not been reported in the literature.

It is interesting to note that adsorbents prepared from the modification of polysaccharides are usually soluble or in a powder form, and so are difficult to separate out after the adsorption process. Contrary to the prior art, we postulate using PS for easy and economical solid–liquid separation. Such an attempt has not been explored previously. In this work, PS was prepared by replacing ice crystals in the frozen starch gel with ethanol using a solvent exchange technique (Qian, Chang, & Ma, 2011) and later modified with carbon disulfide (CD) and citric acid (CA) at low concentrations of NaOH or without NaOH. Subsequently, the adsorption patterns of $Pb^{2+}$ ions by PSX and PSC were characterized.

## 2. Materials and methods

### 2.1. Materials

Potato starch was purchased from Manitoba Starch Products (Manitoba, Canada). Ethanol, carbon disulfide, citric acid and other chemicals were all analytical grade.

### 2.2. Preparation of porous starch (PS)

The preparation of PS was based on the method of Chang, Yu, and Ma (2011). Potato starch (5 g) was added to 100 mL of distilled water and heated at 90 °C for 0.5 h to completely gelatinize the starch. The mixture was refrigerated for a few days at 5 °C until a

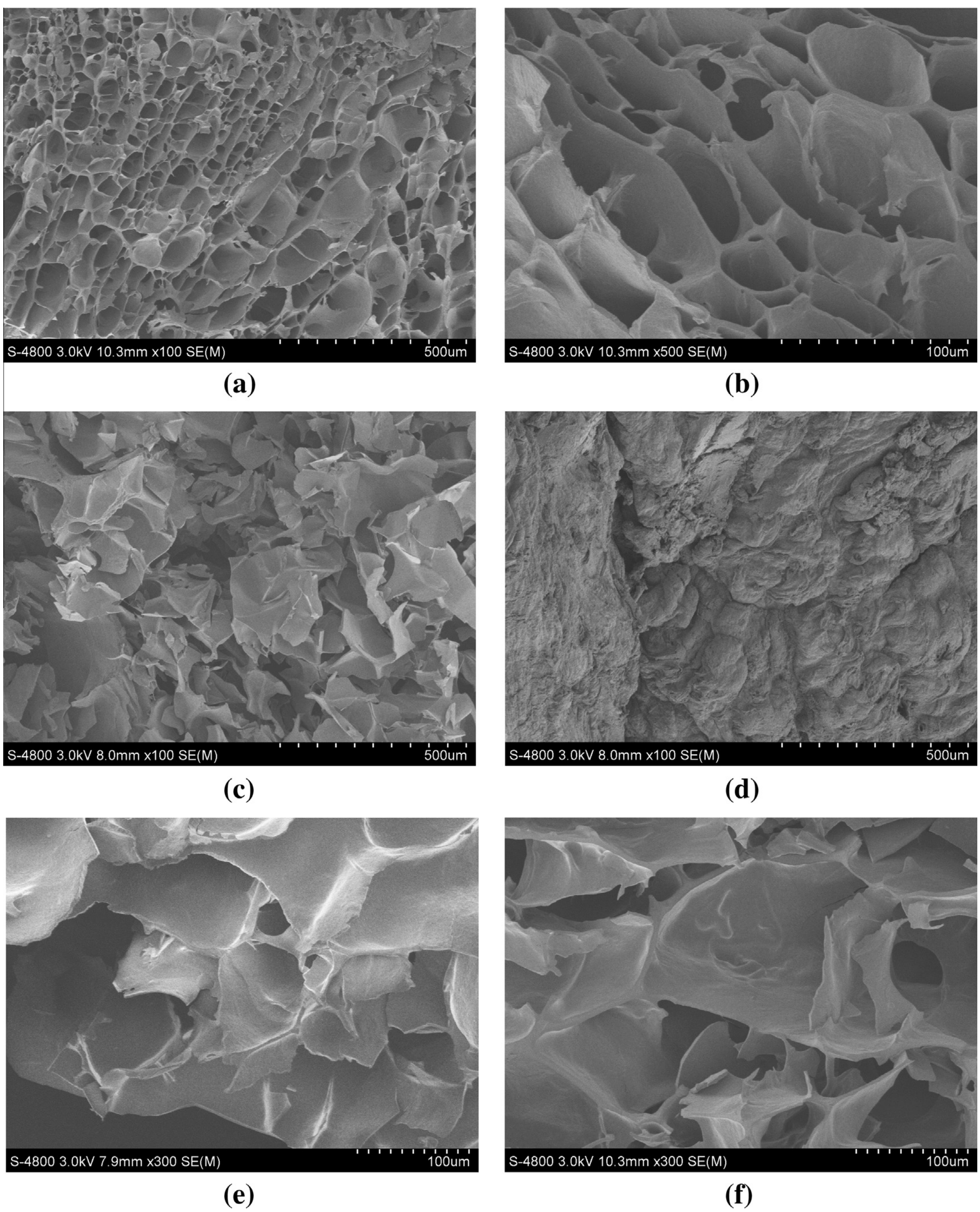


**Fig. 1.** SEM images of PSX1.35 prepared from 0.5% NaOH (a and b); PSX0.54 prepared from 5% NaOH (c); PSX1.35 prepared from 5% NaOH (d); PSC0.1 (e); and PSC1.0. (f).

starch gel formed. The obtained gel was cut into cubes (about 1 × 1 × 1 cm), and frozen. The frozen cubes were immersed in ethanol three times for about 2 h each time. The cubes were then dried at 50 °C for 3 h to remove the ethanol, and white solid PS cubes with a low apparent density of about 90 mg/cm$^3$ were obtained.

### 2.3. Preparation of porous starch xanthate (PSX) and porous starch citrate (PSC)

1 g PS was immersed in 50 mL NaOH solution (0.5% or 5%), and carbon disulfide (0.2, 0.3, 0.4 or 0.5 mL) was added with vigorous stirring. The reaction was processed at 30 °C for 1.5 h. Since the molar mass of starch (i.e., anhydroglucose unit) is 162, the mole ratios of CD/starch were 0.54, 0.81, 1.08 and 1.35, respectively. The obtained PSXs were washed in water three times, and then washed with ethanol three times and dried for testing. PSXs with different CD/starch mole ratios were labeled as: PSX0.54, PSX0.81, PSX1.08, and PSX1.35.

Ethanol solution was used to dissolve CA and disperse the PS cubes. The suspensions were then conditioned for 12 h at room temperature to ensure their homogeneity. The molar ratios of CA and PS were 0.1, 0.2, 0.4, 0.6, 0.8 and 1, respectively. The cubes were dried at 110 °C for 4 h in a forced air oven. The PSCs were immersed in ethanol three times to remove the remaining CA, and then dried. The PSCs with different mole ratios of CA/starch were labeled as: PSC0.1, PSC0.2, PSC0.4, PSC0.6, PSC0.8 and PSC1.0.

Granular potato starch was modified by reacting it with CD or CA to serve as the control.

### 2.4. Scanning electron microscopy (SEM)

The fracture surfaces of PSX and PSC were examined using a Hitachi S-4800 scanning electron microscope. PSX and PSC were cooled in liquid nitrogen and then broken, and the fracture surfaces were vacuum coated with gold for SEM.

### 2.5. Fourier transform infrared spectroscopy (FTIR)

FTIR analysis of PSX or PSC was performed at 2 cm$^{-1}$ resolution on a Bio-Rad FTS 3000 IR Spectrum Scanner. Samples were prepared by making pellets with dried IR grade KBr and, typically, 64 scans were signal-averaged to reduce spectral noise.

### 2.6. Adsorption experiments

Adsorption experiments were conducted using glass bottles containing 2 g/L of the adsorbents and $PbNO_3$ solution (0.5 g/L $Pb^{2+}$). The glass bottles were placed on a slow-moving platform shaker for a certain length of time during the adsorption process. To investigate the effect of the mole ratio on equilibrium adsorption capacity, the $Pb^{2+}$ concentrations were tested after the adsorbents were in the $PbNO_3$ solution for 2 h. The $Pb^{2+}$ concentrations in the solutions were analyzed using an atomic adsorption spectrometer (Thermo Scientific iCE 3000) to determine the amount of $Pb^{2+}$ adsorbed at 30 °C. The solution had to pass through a filter membrane to remove the soluble starch components before testing for granular starch xanthate.

The adsorption isotherm, where the concentration of the adsorbent was 2 g/L and the $Pb^{2+}$ concentration changed from 0.5 to 1.5 g/L, was studied as well. These experiments were carried out at 30 °C and the bottles were shaken on a rotary shaker at 100 rpm for 2 h to reach the adsorption equilibrium.

## 3. Results and discussion

### 3.1. Morphology of PSX and PSC

As shown in Fig. 1(a and b), the porous structure was not destroyed during CD modification, even with a high CD/starch mole ratio, when the NaOH concentration was low (0.5%). However, when the NaOH concentration was 5%, the porous structure was partly destroyed when the CD/starch mole ratio was low (0.54), as revealed in Fig. 1(c). When the CD/starch mole ratio was 1.35, the walls of the porous starch were soluble in 5% NaOH solution and the porous structure completely disappeared (Fig. 1(d)). The reaction between starch and CD in the presence of NaOH is:

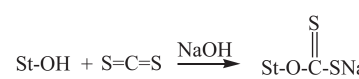

NaOH weakens the intermolecular interactions of the starch molecules and facilitates the reaction between starch and CD. A concentrated NaOH solution, however, may lead to the degradation and solubilization of starch.

The morphology of PSC is shown in Fig. 1(e and f). With an increase in the CA/starch mole ratio from 0.1 to 1.0, the porous structure was maintained. CA modification of PS was a crosslinking reaction (Ma, Chang, Yu, & Stumborg, 2009), which facilitated the stability of the porous structures. The following reaction exhibits the modification of porous starch with CA:

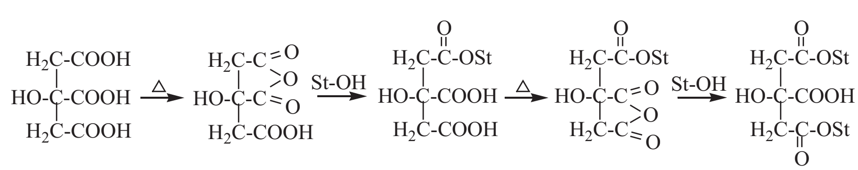

### 3.2. FTIR of PSX and PSC

Fig. 2 shows the FTIR spectra of PSX and PSC. For PS in Fig. 2(a), the band at about 3400 cm$^{-1}$ was attributed to the hydrogen-bonded hydroxyl groups of starch. The peak at about 1160 cm$^{-1}$ was related to C—O bond stretching of the C—O—H group, and the peaks at 1080 and 1020 cm$^{-1}$ were ascribed to C—O bond stretching of the C—O—C group in the anhydroglucose ring (Chang, Qian, Anderson, & Ma, 2012). The three characteristic absorption peaks of the —(C=S)—S—H group appeared in the ranges of 1250–1200, 1140–1110, and 1070–1020 cm$^{-1}$ (Chang, Hao, & Duan, 2008; Lu, Xiao, & Sun, 2012). The band from the C—O bond stretching in starch and the characteristic peak of xanthate groups may overlap in PSX. The formation of xanthate groups resulted in a change in the relative intensity and location of three peaks in the range of 1200–1000 $cm^{-1}$ and the more diffuse bands of the hydrogen-bonded hydroxyl groups of starch in the 3200–3600 $cm^{-1}$ range. Similarly, Deng et al. (2012) confirmed the occurrence of a sulfonation reaction by the change in relative intensity of the three characteristic peaks between 1200 and 1000 $cm^{-1}$.

As illustrated in Fig. 2(b), absorption bands due to the C═O stretching of esters were observed at 1730 $cm^{-1}$ (Yoshimura, Yoshimura, Seki, & Fujioka, 2006) in PSC. This absorption peak was absent in PS which indicated the formation of esters by the reaction between the hydroxyl group in the porous starch and the carboxylic anhydride group in CA. The peak intensity obviously increased with increased CA/starch mole ratios (from 0.1 to 1). The relative intensity and peak location of the C—O bond stretching of starch also changed in the 1200–1000 $cm^{-1}$ range.

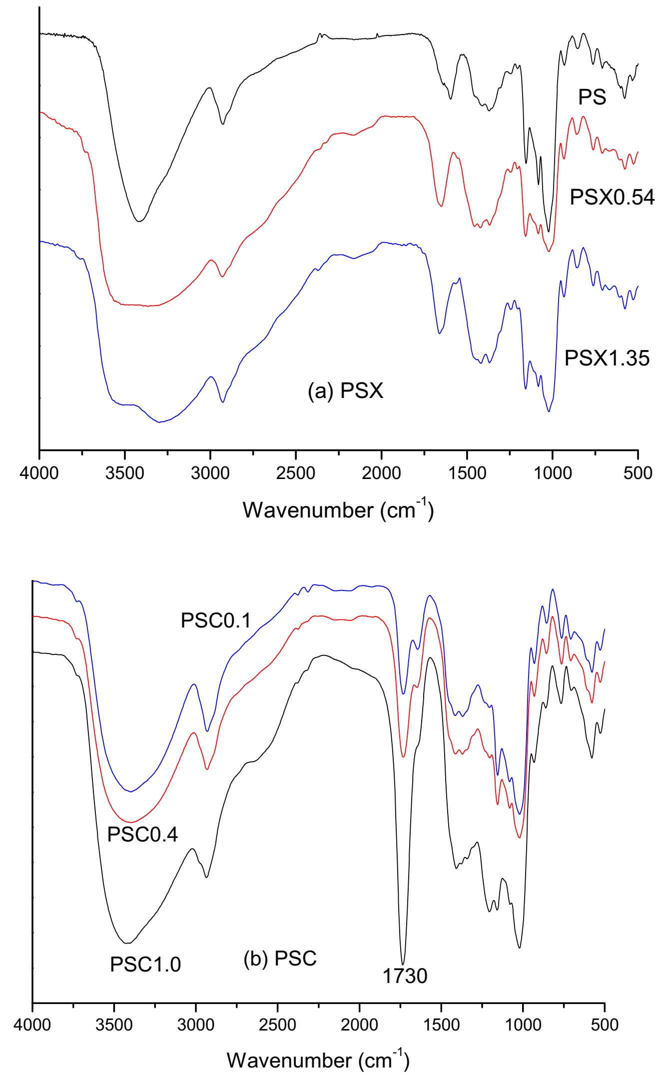


**Fig. 2.** The FT-IR spectra of (a) PSXs prepared with different mole ratios of CD/starch and (b) PSCs prepared with different mole ratios of CA/starch.

### 3.3. Effect of mole ratio on equilibrium adsorption capacity

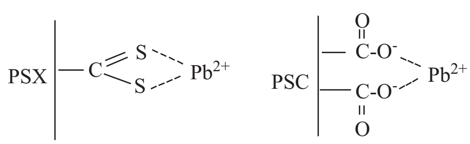


The mechanism of $Pb^{2+}$ adsorption by PSX and PSC is illustrated above. Presumably, xanthate and carboxylate groups on the walls of porous starch anchor chelation and electrostatic interactions with heavy metal ions. Indeed, chelation between xanthate and $Pb^{2+}$ ions removed $Pb^{2+}$ from water, while the carboxylate formed electrostatic interactions with $Pb^{2+}$ ions. One xanthate group can remove one $Pb^{2+}$ ion, while it takes two carboxylate groups to adsorb one $Pb^{2+}$ ion. This indicates that chelation allows PSX to adsorb more $Pb^{2+}$ than the electrostatic interaction between PSC and $Pb^{2+}$. The mole ratio of CD/starch and CA/starch affected the numbers of xanthate and carboxylate groups on the walls of the porous starch, which then determined the equilibrium adsorption capacity of PSX and PSC.

The dependence of the equilibrium adsorption capacity of $Pb^{2+}$ on the CD/starch mole ratio is shown in Fig. 3(a). For PSX from 0.5% NaOH, the equilibrium adsorption capacity of $Pb^{2+}$ increased with increasing CD/starch mole ratio, and reached 103.6 mg/g at the CD/starch mole ratio of 1.35. The adsorption capacity of granular starch xanthate exhibited a similar dependence on the CD/starch mole ratio, while PSX from 5% NaOH displayed an adsorption capacity as high as 155.0 mg/g at a CD/starch mole ratio of 1.35. However, PSXs from 5% NaOH were soluble in water and therefore not easily separated. Granular starch xanthate was also partly soluble; therefore, PSX1.35 was investigated for batch adsorption kinetics and isotherm without separation treatment.

The effect of the CA/starch mole ratio on the equilibrium adsorption capacity of $Pb^{2+}$ is illustrated in Fig. 3(b). When the CA/starch mole ratio increased from 0.1 to 1.0, the amount of $Pb^{2+}$ adsorbed at equilibrium increased for both PSC and granular starch citrate. The newly grafted carboxylate groups brought negatively charged sorption sites and formed an electrostatic attraction with the positively charged ions (Huang, Bu, Jiang, & Zeng, 2011). Because starch granules and crystallinity were destroyed during starch gelatinization, the large specific surface areas of PS facilitated CA modification and more carboxylate groups formed on the walls of PSCs, which exhibited a higher equilibrium adsorption capacity than granular starch citrate. When the CD/starch mole ratio was 1.0, the adsorption capacity for $Pb^{2+}$ on PSC1.0 was 47.0 mg/g.

### 3.4. Batch adsorption kinetics

Fig. 4(a) reveals the effect of contact time on adsorption of $Pb^{2+}$ by PSX1.35 and by PSC1.0. The uptake of $Pb^{2+}$ by PSX1.35 was high and rather fast. The adsorption equilibrium from the experimental curve was 103.6 mg/g after only 20 min for PSX1.35, while for PSC1.0 the amount of dye adsorbed at equilibrium was 47.0 mg/g after 60 min.

The kinetic models of pseudo-second-order and intraparticle diffusion were used to investigate adsorption kinetics by PSX1.35 or PSC1.0. According to the pseudo second-order model, the amount of $Pb^{2+}$ adsorbed at any time, $t$ (min), is expressed as Eq. (1):

$$\frac{t}{q_t} = \frac{1}{kq_e^2} + \frac{t}{q_e} \qquad (1)$$

where $q_t$ (mg/g) and $q_e$ (mg/g) represent the amounts of dye adsorbed at any time $t$ (min) and at equilibrium, respectively, and $k$ (mg/g min) is the second-order rate constant.

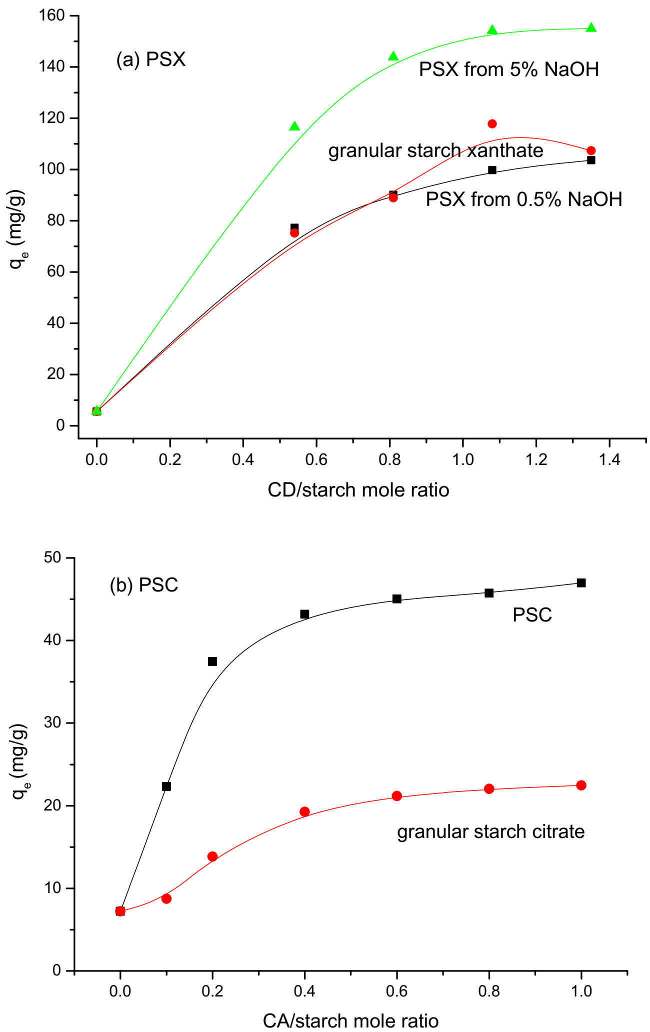


**Fig. 3.** Effect of mole ratio of (a) CD/starch and (b) CA/starch on equilibrium adsorption capacity of $Pb^{2+}$ by PSXs and PSCs. Initial concentrations: $Pb^{2+}$ 0.5 g/L; adsorbent 2 g/L.

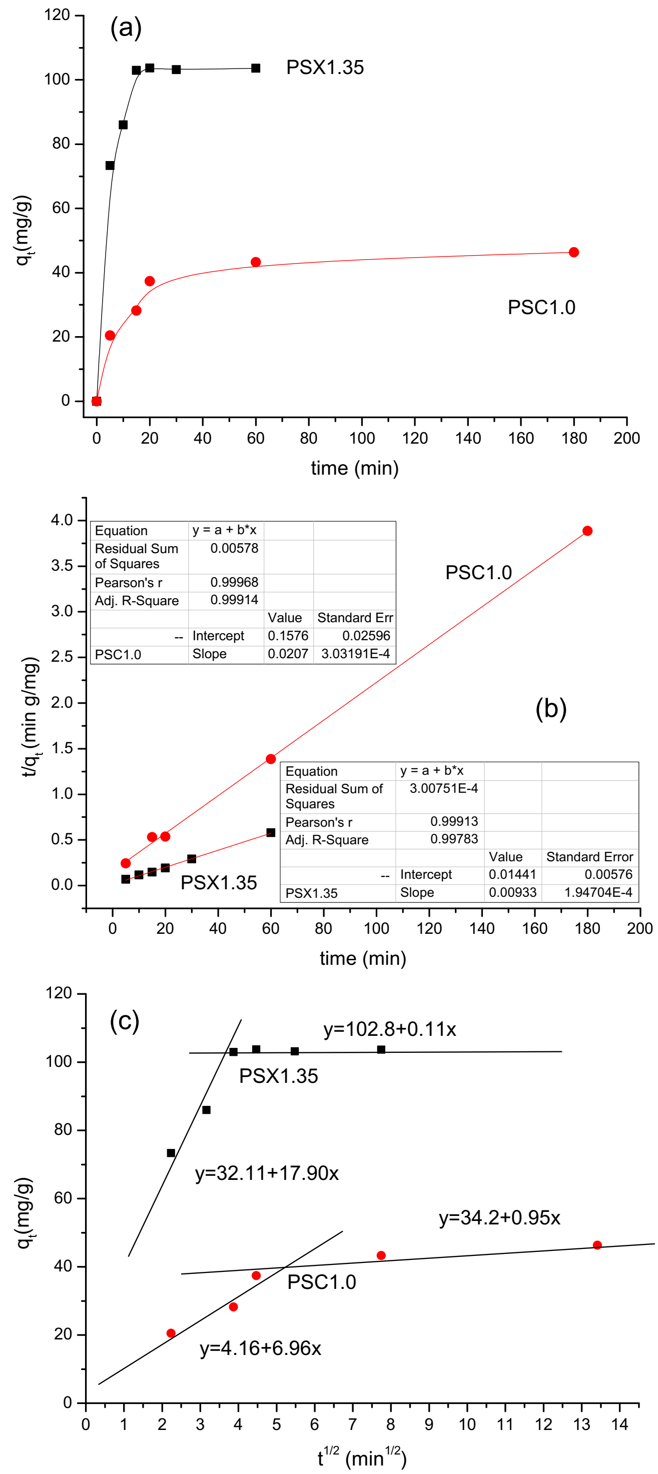


**Fig. 4.** Effect of contact time on adsorption of $Pb^{2+}$ by PSX1.35 and PSC1.0 (a); the pseudo-second-order model (b) and intra-particle model (c) for batch adsorption of $Pb^{2+}$. Initial concentrations: $Pb^{2+}$ 0.5 g/L; adsorbent 2 g/L.

Fig. 4(b) shows the relationship between $t/q_t$ and $t$. Some kinetic parameters ($k$ and $q_e$) were calculated from the intercept and slope of the line in a $t/q_t$ versus $t$ plot, and are listed in Table 1. There were linear relationships with high correlation coefficients ($R > 0.999$) between $t/q_t$ and $t$ for both PSX1.35 and PSC1.0, which indicated that the adsorption process fit the pseudo second-order model well. In terms of $q_e$, PSX1.35 exhibited better adsorption of $Pb^{2+}$ (107.2 mg/g) than PSC1.0 (48.3 mg/g).

The intra-particle diffusion model, expressed in Eq. (2), was used to investigate the diffusion mechanism of the adsorption process,

$$q_t = K_{id}t^{1/2} + C \tag{2}$$

where $K_{id}$ (mg/g min$^{1/2}$) is the intra-particle diffusion rate constant and $C$ is the intercept.

As shown in Fig. 4(c), the plot can be divided into two consecutive steps: (1) the external diffusion stage depicting macro-pore diffusion; and (2) the gradual adsorption until equilibrium is reached, where the adsorption is controlled by micro-pore diffusion (Ding et al., 2013). The rate constants $K_{id}$ and $C$ are shown in Table 1. For both PSX1.35 and PSC1.0, $K_{id1}$ was much larger than $K_{id2}$. This indicated that micro-pore diffusion was the main rate-limiting step in the adsorption process, but not the sole rate-limiting step. Comparatively, the macro-pore diffusion of PSC1.0 may control the adsorption kinetics more than that of PSX1.35.

### 3.5. Batch adsorption isotherm

Adsorption isotherms were studied using Langmuir's isotherm model, described as Eq. (3).

**Table 1**
Kinetic constants and isothermal constants for $Pb^{2+}$ adsorption by PSX1.35 and PSC1.0 at 30 °C.

| | Pseudo-second-order model | | | Experimental $q_e$ (mg/g) | Intra-particle diffusion model | | | | Langmuir constants | | |
|---|---|---|---|---|---|---|---|---|---|---|---|
| | | | | | First stage | | Second stage | | | | |
| | $k$ (g/mg min) | $q_e$ (mg/g) | $R$ | | $K_{id1}$ (mg/g min$^{1/2}$) | $C_1$ | $K_{id2}$ (mg/g min$^{1/2}$) | $C_2$ | $b$ (L/mg) | $Q_{max}$ (mg/g) | $R$ |
| PSX1.35 | 0.0060 | 107.2 | 0.9991 | 103.6 | 17.90 | 32.11 | 0.11 | 102.8 | 0.158 | 109.1 | 0.9999 |
| PSC1.0 | 0.0027 | 48.3 | 0.9996 | 47.0 | 6.96 | 4.16 | 0.95 | 34.2 | 0.008 | 57.6 | 0.9961 |

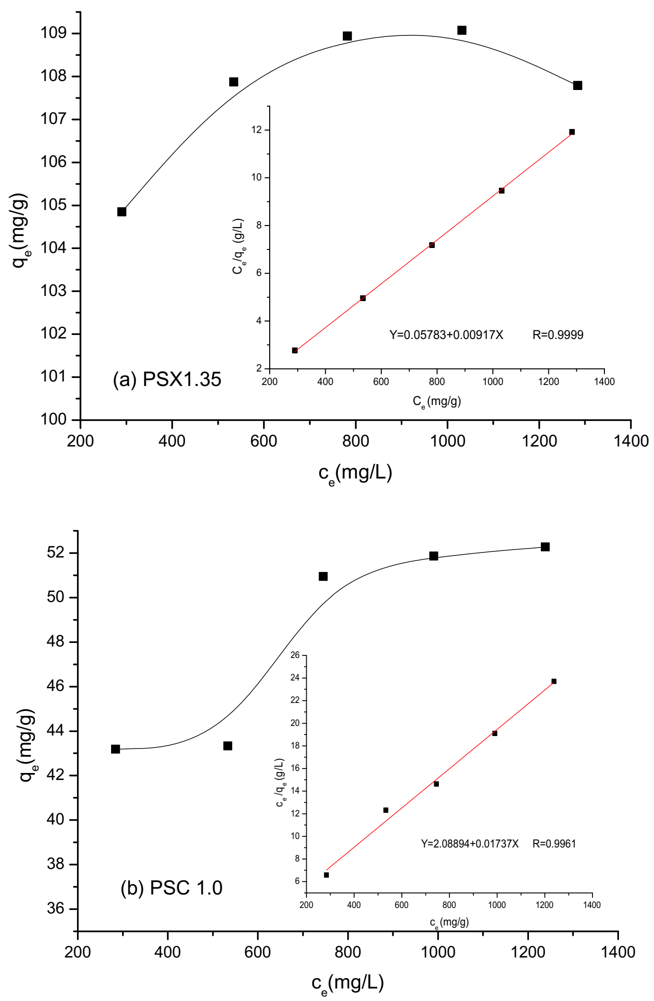


**Fig. 5.** Adsorption isotherms of (a) $Pb^{2+}$ by PSX1.35 and (b) PSC1.0 at 30 °C. Inset is the Langmuir model mode for adsorption of $Pb^{2+}$ by PSX1.35 and PSC1.0.

$$\frac{c_e}{q_e} = \frac{1}{bQ_{max}} + \frac{c_e}{Q_{max}} \tag{3}$$

where $q_e$ (mg/g) is the equilibrium adsorption capacity; $c_e$ (mg/L) is the equilibrium concentration in the solution; $Q_{max}$ (mg/g) is the maximum adsorption capacity; and $b$ (L/mg) is the binding constant of Langmuir adsorption.

The Langmuir isotherm plots for PSX1.35 and PSC1.0 are shown in Fig. 5(a and b), respectively, and the parameters are exhibited in Table 1. The adsorption of PSX1.35 and PSC1.0 fit the Langmuir model well because $R$ was very close to 1. In the Langmuir isotherm model, $b$ is related to the bonding energy coefficient. The value of $b$ for PSX1.35 was 0.158 L/mg, which was larger than that for PSC1.0 (0.008 L/mg) indicating that PSX1.35 had higher affinity for $Pb^{2+}$ ions than PSC1.0. The chelation interaction between the xanthate group and $Pb^{2+}$ ion was stronger than the electrostatic interaction between the carboxylate group and $Pb^{2+}$ ion. Similarly, the binding constant, b, was used to estimate the interaction between adsorbent and adsorbate (Ma, Chang, Zheng, Zhao, & Ma, 2014). The maximum monolayer adsorption capacities of $Pb^{2+}$ ions were 109.1 and 57.6 mg/g for PSX1.35 and PSC1.0, respectively. The $Pb^{2+}$ $Q_{max}$ values for PSX1.35 and PSC1.0 were competitive with the $Pb^{2+}$ adsorption capacities of other adsorbents from polysaccharides, including xanthate-modified magnetic chitosan (76.9 mg/g) (Zhu, Hu, & Wang, 2012); $Pb^{2+}$ imprinted chitosan bead (79.2 mg/g) (Lu, He, & Luo, 2013); thiol-functionalized cotton, wood sawdust, and buckwheat hull (28.67, 43.14 and 44.84 mg/g) (Wu, Cheng, & Ma, 2012); and crosslinked carboxymethyl starch (80 mg/g) (Chen, Zhong, & Fang, 2012).

## 4. Conclusion

Starch xanthate and starch citrate with porous structures were successfully prepared in a simple modification process, owing to the ample specific surface area available for chemical modification on PS. Interestingly, $Pb^{2+}$ ions quickly diffused to the functionalized walls (due to the attached xanthate and carboxylate groups) of PS through the open pore structure. The CD/starch and CA/starch mole ratios had a great effect on the adsorption capacity of PSXs and PSCs for the $Pb^{2+}$ ion. This adsorption process could be described well by the pseudo-second-order kinetic model and the Langmuir isotherm model. The maximum adsorption capacities of PSX1.35 and PSC1.0 were 109.1 and 57.6 mg/g, respectively.

The innovation disclosed here is starch-based (an environmentally friendly, economical, and renewable bio-resource), scalable (-suitable for industrial production), and applicable to industrial applications. The potential applications for modified PS, i.e., PSX and PSC, can be extended to wastewater treatment, metal recovery, agri-food, pharmaceuticals, and so on.

## References


Altun, T., & Pehlivan, E. (2012). Removal of Cr(VI) from aqueous solutions by modified walnut shells. *Food Chemistry, 132*, 693–700.

Chang, Q., Hao, X. K., & Duan, L. L. (2008). Synthesis of crosslinked starch-graft-polyacrylamide-*co*-sodium xanthate and its performances in wastewater treatment. *Journal of Hazardous Materials, 159*, 548–553.

Chang, P. R., Qian, D. Y., Anderson, D. P., & Ma, X. F. (2012). Preparation and properties of the succinic ester of porous starch. *Carbohydrate Polymers, 88*, 604–608.

Chang, P. R., Yu, J. G., & Ma, X. F. (2011). Preparation of porous starch and its use as a structure-directing agent for production of porous zinc oxide. *Carbohydrate Polymers, 83*, 1016–1019.

Chen, Y. X., Zhong, B. H., & Fang, W. M. (2012). Adsorption characterization of lead(II) and cadmium(II) on crosslinked carboxymethyl starch. *Journal of Applied Polymer Science, 124*, 5010–5020.

Deng, L., Geng, M. J., Zhu, D. W., Zhou, W. B., Langdon, A., Wu, H. W., et al. (2012). Effect of chemical and biological degumming on the adsorption of heavy metal by cellulose xanthogenates prepared from *Eichhornia crassipes*. *Bioresource Technology, 107*, 41–45.

Ding, D. H., Zhao, Y. X., Yang, S. J., Shi, W. S., Zhang, Z. Y., Lei, Z. F., et al. (2013). Adsorption of cesium from aqueous solution using agricultural residue – Walnut shell: Equilibrium, kinetic and thermodynamic modeling studies. *Water Research, 47*, 2563–2571.

Dong, A. Q., Xie, J., Wang, W. M., Yu, L. P., Liu, Q., & Yin, Y. P. (2010). A novel method for amino starch preparation and its adsorption for Cu(II) and Cr(VI). *Journal of Hazardous Materials, 181*, 448–454.

Huang, X. Y., Bu, H. T., Jiang, G. B., & Zeng, M. H. (2011). Cross-linked succinyl chitosan as an adsorbent for the removal of methylene blue from aqueous solution. *International Journal of Biological Macromolecules, 49*, 643–651.

Jain, M., Garg, V. K., & Kadirvelu, K. (2009). Chromium(VI) removal from aqueous system using *Helianthus annuus* (sunflower) stem waste. *Journal of Hazardous Materials, 162*, 365–372.

Kaya, K., Pehlivan, E., Schmidt, C., & Bahadie, M. (2014). Use of modified wheat bran for the removal of chromium(VI) from aqueous solutions. *Food Chemistry, 158*, 112–117.

Liu, F., Luo, X. G., Lin, X. Y., Liang, L., & Chen, Y. (2009). Removal of copper and lead from aqueous solution by carboxylic acid functionalized deacetylated konjac glucomannan. *Journal of Hazardous Materials, 171*, 802–808.

Lu, Y. C., He, J., & Luo, G. S. (2013). An improved synthesis of chitosan bead for Pb(II) adsorption. *Chemical Engineering Journal, 226*, 271–278.

Lu, D. R., Xiao, C. M., & Sun, F. (2012). Controlled grafting of poly(vinyl acetate) onto starch via RAFT polymerization. *Journal of Applied Polymer Science, 124*, 3450–3455.

Ma, X. F., Chang, P. R., Yu, J. G., & Stumborg, M. (2009). Properties of biodegradable citric acid-modified granular starch/thermoplastic pea starch composites. *Carbohydrate Polymers, 75*, 1–8.

Ma, T. T., Chang, P. R., Zheng, P. W., Zhao, F., & Ma, X. F. (2014). Fabrication of ultra-light graphene-based gels and their adsorption of methylene blue. *Chemical Engineering Journal, 240*, 596–600.

Qian, D. Y., Chang, P. R., & Ma, X. F. (2011). Preparation of controllable porous starch with different starch concentrations by the single or dual freezing process. *Carbohydrate Polymers, 86*, 1181–1186.

Ren, Y., Abbood, H. A., He, F. B., Peng, H., & Huang, K. X. (2013). Magnetic EDTA-modified chitosan/$SiO_2$/$Fe_3O_4$ adsorbent: Preparation, characterization, and application in heavy metal adsorption. *Chemical Engineering Journal, 226*, 300–311.

Sdiri, A., Higashi, T., Chaabouni, R., & Jamoussi, F. (2012). Competitive removal of heavy metals from aqueous solutions by montmorillonitic and calcareous clays. *Water, Air, and Soil Pollution, 223*, 1191–1204.

Tofighy, M. A., & Mohammadi, T. (2011). Adsorption of divalent heavy metal ions from water using carbon nanotube sheets. *Journal of Hazardous Materials, 185*, 140–147.

Wang, Z. D., Yin, P., Qu, R. J., Chen, H., Wang, C. H., & Ren, S. H. (2013b). Adsorption kinetics, thermodynamics and isotherm of Hg(II) from aqueous solutions using buckwheat hulls from Jiaodong of China. *Food Chemistry, 136*, 1508–1514.

Wang, H., Yuan, X. Z., Wu, Y., Huang, H. J., Zeng, G. M., Liu, Y., et al. (2013a). Adsorption characteristics and behaviors of graphene oxide for Zn(II) removal from aqueous solution. *Applied Surface Science, 279*, 432–440.

Wang, F. C., Zhao, J. M., Wei, X. T., Huo, F., Li, W. S., Hu, Q. Y., et al. (2014). Adsorption of rare earths (III) by calcium alginate-poly glutamic acid hybrid gels. *Journal of Chemical Technology and Biotechnology, 89*, 969–977.

Wu, Z. M., Cheng, Z. H., & Ma, W. (2012). Adsorption of Pb(II) from glucose solution on thiol-functionalized cellulosic biomass. *Bioresource Technology, 104*, 807–809.

Yoshimura, T., Yoshimura, R., Seki, C., & Fujioka, R. (2006). Synthesis and characterization of biodegradable hydrogels based on starch and succinic anhydride. *Carbohydrate Polymers, 64*, 345–349.

Zhu, Y., Hu, J., & Wang, J. (2012). Competitive adsorption of Pb(II), Cu(II) and Zn(II) onto xanthate-modified magnetic chitosan. *Journal of Hazardous Materials, 221–222*, 155–161.